Magnetic Tunnel Junctions with a Composite Free Layer: A New Concept for Future Universal Memory

A. Makarov, V. Sverdlov, and S. Selberherr
Institute for Microelectronics, TU Wien, A-1040 Vienna, Austria

1. Introduction

In modern microelectronic devices the dominant memory types are DRAM, static RAM, and flash memory. These types of memory store data as a charge state. For many decades these memory technologies have been successfully scaled down to achieve higher speed and increased density of memory chips at lower bit cost.[1] However, memories based on charge storage are gradually approaching the physical limits of scalability and conceptually new types of memory based on a different storage principle are gaining momentum.

Memories based on magnetic moment storage form an important sub-class of the non-volatile memories based on new physical principles.[2] Magnetic memory technologies include magnetoresistive random access memory (MRAM), spin transfer torque RAM (STT-MRAM), and racetrack memory,[3] although the latter is still in the conceptual stage. Recent advances in STT-MRAM technology makes this type of memory a promising candidate for future universal memory, combining nonvolatility, fast operation, and low power consumption. In this chapter, we will focus our attention on MRAM and STT-MRAM.

2. Magnetic memory technologies

The basic element of an MRAM is a sandwich of two magnetic layers separated either by a nonmagnetic metal in giant magnetoresistance (GMR) devices, or by a thin insulating oxide in magnetic tunnel junction (MTJ) devices – see Fig. 1. While the magnetization of the pinned layer is fixed due to the fabrication process, the magnetization direction of the free layer can be switched between the two states parallel and anti-parallel to the fixed magnetization direction.

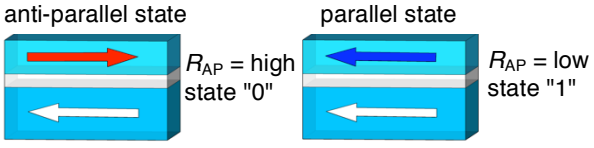

Figure 1. Schematic illustration of a three-layer MTJ in a high-resistance state (left) and low-resistance state (right).

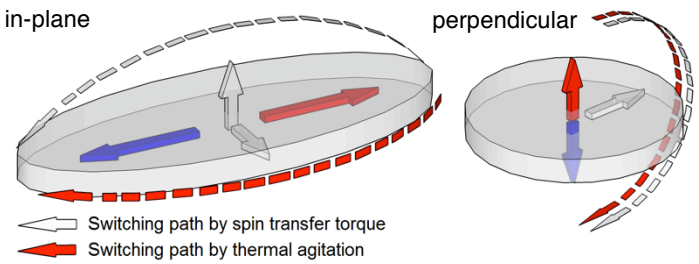

Figure 2. Schematic illustration of the free layer with an "in-plane" magnetization (left) and “perpendicular" magnetization direction (right).

Depending on the orientation of the magnetizations the magnetic pillars can be divided into two categories: "in-plane" with magnetization lying in the plane of the magnetic layer and "perpendicular" with out-of-plane magnetization direction.

In a conventional field-driven MRAM cell, switching the magnetization of a free layer is performed by applying a magnetic field. In contrast to field-driven MRAM, STT-MRAM does not require an external magnetic field. Instead, switching between the two states occurs due to spin transfer torque arising from the spin-polarized current flowing through the pillar. The theoretical prediction of the spin transfer torque effect was made independently by Slonczewski and Berger.[4,5] When electrons pass through the thick magnetic layer, the spins of the electrons become aligned with the magnetization of the fixed layer. When these spin-polarized electrons enter the free layer, their spin orientations align with the magnetization of the free layer within a transition length of a few Å. Because of their spin reorientation, they exert a torque on the magnetization of the free layer, which can cause magnetization switching, if the torque is large enough to overcome damping. Smaller torque values result in magnetization precession around the effective magnetic field.

The spin-polarized current is only a fraction of the total charge current flowing through the device. Therefore, high current densities from ~10^7 to ~10^8 A/cm^2 are required to switch the magnetization direction of the free layer, and the reduction of this current density is the most important technological challenge in this area.

Switching of the magnetization can occur not only under the influence of the spin-polarized current, but also spontaneously, due to thermal fluctuations – see Fig. 2. This is an unwanted event that leads to the loss of stored information. Thus another important parameter of MRAM (STT-MRAM) is the thermal stability factor, defined as the ratio of the thermal stability barrier to the operating temperature.

The thermal stability factor Δ_{PERP}[6,7] for perpendicular MTJs (p-MTJs) is given by the interface-induced perpendicular anisotropy field H_K^{perp} as

$$\Delta_{PERP} = \frac{M_S \cdot \left(H_K^{perp} - 4\pi M_S\right) \cdot V}{2k_B T} \quad , \qquad (1)$$

where M_S is the saturation magnetization, V is the volume of the free layer, and k_B is the Boltzmann constant. To increase the thermal stability factor it is sufficient to increase the cross-section of p-MTJs. However, due to domain formation, this is limited to approximately 70 nm diameter, and therefore increasing the thermal stability factor of p-MTJs above ~40–50 remains a challenge.[8]

In p-MTJs the switching paths by spin transfer torque and thermal agitation are the same, as shown in Fig. 2 (right). Thus, the critical switching currents for p-MTJs are proportional to the thermal stability factor.

The thermal stability factor Δ_{INP}[6,7] for in-plane MTJs is determined by the shape anisotropy field H_K^{inp}:

$$\Delta_{INP} = \frac{M_S \cdot H_K^{inp} \cdot V}{2k_B T} \quad . \tag{2}$$

To increase the in-plane thermal stability factor it is sufficient to increase the thickness of the free layer and/or the aspect ratio. However, switching under the influence of the spin current follows a different path from thermal agitation switching, as shown in Fig. 2 (left). This leads to a large additional $2\pi M_S^2 V$ term in the switching current:

$$J_C^{inp} \sim M_S \cdot V \cdot \left(H_K^{inp} + 2\pi M_S\right) = 2k_B T \Delta_{INP} + 2\pi M_S^2 V \,, \tag{3}$$

which results in a higher critical current density compared to that in p-MTJs.[6,7]

Therefore, the in-plane MTJs exhibit a high thermal stability, but still require a reduction of the critical current density. Perpendicular MTJs with an interface-induced anisotropy show potential, but still require a reduction of damping and an increase in thermal stability. Thus, further research in new materials and architectures for MTJ structures is urgently needed.

3. MTJs with a composite free layer

We have recently proposed a five-layer MTJ with a composite free layer.[9] The composite magnetic layer consists of two half-ellipses separated by a non-magnetic spacer, as shown in Fig. 3. The magnetization of the magnetic layers lies in the plane. Compared to p-MTJs, the composite free layer his broadens substantially the range of the magnetic materials suited for constructing MTJs. Below we examine the switching characteristics of these structures.

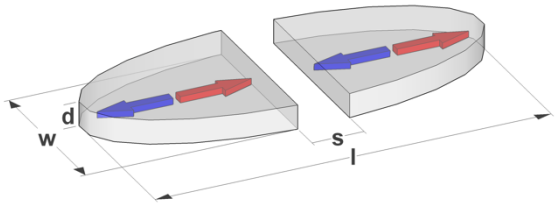

Figure 3. Schematic illustration of the composite free layer.

- *Thermal stability and thermal agitation switching*

To find the switching path due to thermal agitations it is necessary to determine the state for which the barrier separating the two stable magnetization states in the free layer is minimal. Figure 4 shows that the switching path due to thermal agitations must go through the state with magnetizations of the halves opposite to each other (the C state in Fig. 4).

We investigated the influence of scaling the dimensions on the thermal stability factor for MTJs with a composite free layer. Due to the removal of the central region in the monolithic structure, the shape anisotropy is slightly decreased together with the thermal stability factor. To boost the thermal stability factor, it is sufficient to increase the thickness of the free layer and/or the aspect ratio. Figure 5 shows the thermal stability factors of MTJs with a composite free layer as a function of the free layer thickness d. An MTJ with 52.5×10 nm^2 cross-section and d = 5 nm free layer thickness has a thermal stability factor ~60, which exceeds all of the p-MTJs demonstrated to date.[8]

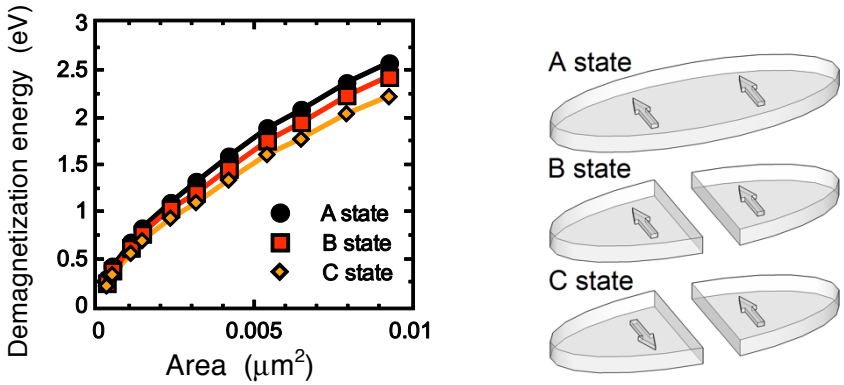

Figure 4. Dependence of the demagnetization energy for MTJs with monolithic (a) and composite (b, c) free layers as a function of the cross-sectional area.

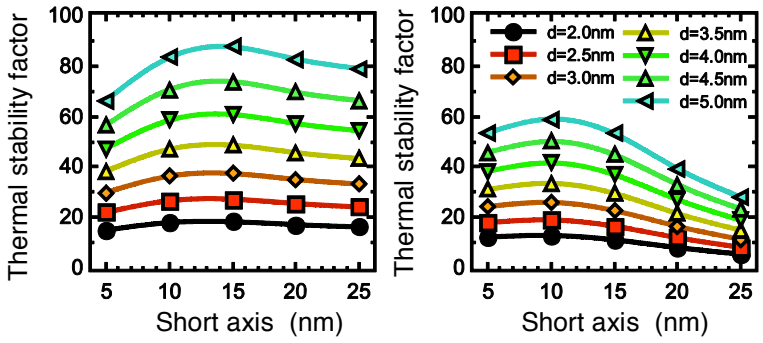

Figure 5. Thermal stability barrier for MTJs with monolithic (left) and composite free layer (right) as a function of the short axis length for several free layer thicknesses d. The long axis is fixed at 52.5 nm; fixed layer thickness layer is 5 nm.

- *Spin transfer torque switching*

Our simulations of five-layer MTJ switching are based on the magnetization dynamics described by the Landau-Lifschitz-Gilbert (LLG) equation with additional spin torque terms:[10]

$$\begin{aligned}\frac{dm}{dt} &= -\frac{\gamma}{1+\alpha^2}\cdot\Big(\big(m\times h_{eff}\big)+\alpha\cdot\big[m\times\big(m\times h_{eff}\big)\big]\\ &+\frac{g\mu_B J}{e\gamma M_S d}\cdot\Big(g(\theta_1)\cdot\big(\alpha\cdot(m\times p_1)-\big[m\times(m\times p_1)\big]\big)\\ &-g(\theta_2)\cdot\big(\alpha\cdot(m\times p_2)-\big[m\times(m\times p_2)\big]\big)\Big)\Big).\end{aligned} \tag{4}$$

Here, $\gamma = 2.3245\times10^5$ m/(A·s) is the gyromagnetic ratio, α is the Gilbert damping parameter, μ_B is the Bohr magneton, J is the current density, e is the electron charge, d is the thickness of the free layer, $m \equiv M/M_S$ is the position-dependent normalized vector of the free layer magnetization, $p_1 = M_{p1}/M_{Sp1}$ and $p_2 = M_{p2}/M_{Sp2}$ are the normalized magnetizations in the first and second pinned layers, and M_S, M_{Sp1}, and M_{Sp2} are the saturation magnetizations of the free, first pinned and second pinned layers respectively. We use Slonczewski's expressions for the MTJ with a dielectric layer:[11]

$$g(\theta) = 0.5\cdot\eta\cdot\left[1+\eta^2\cdot\cos(\theta)\right]^{-1}. \tag{5}$$

The local effective field is calculated as:

$$H_{EFF} = H_{EXT} + H_{ANI} + H_{EX} + H_{DMAG} + H_{TH} + H_{AMP} + H_{MS}\ , \tag{6}$$

where H_{EXT} is the external field, H_{ANI} is the magnetic anisotropy field, H_{EX} is the exchange field, H_{DMAG} is the demagnetizing field, H_{TH} is the thermal field, H_{AMP} is the Ampere field, and H_{MS} is the magnetostatic coupling between the pinned and the free layers.

For demonstration of the current-induced switching we look at the magnetization dynamics of the left and right part of the composite free layer separately, see Fig. 6. We consider a structure with an elliptical 52.5×25 nm^2 cross-section and the following layer sequence: 5 nm CoFeB / 1 nm MgO / 2 nm CoFeB / 1 nm MgO / 5 nm CoFeB. The central 2.5 nm stripe is removed from the middle CoFeB layer. Figures 6(b) and (c) show that the switching processes of the left and right parts of the composite free layer occur in opposite senses to each other. Thus, the switching path is similar to that due to thermal agitation. This fact means that, as in p-MTJs, the switching barrier in an MTJ with a composite free layer becomes practically equal to the thermal stability barrier.

To further prove this, we compare the height of the thermal energy barrier with that of the switching energy barrier. Figure 7 shows simulation results for MTJs with a composite free layer and 52.5×10 nm^2 cross-section, as a function of the free layer thickness d. We observe that the barriers are very close to each other for a broad range of free layer thicknesses.

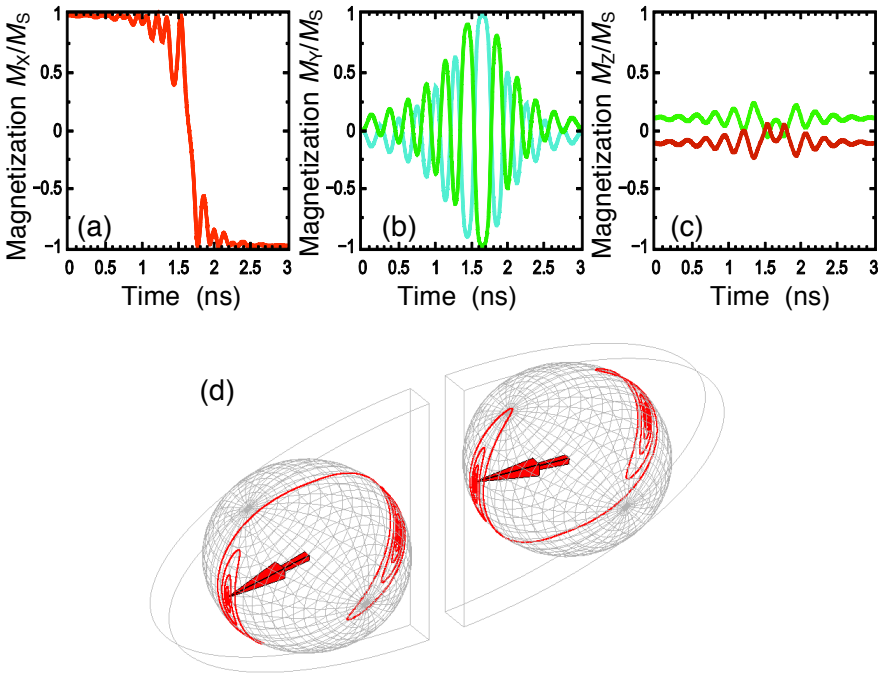

Figure 6. Magnetization components *vs.* time for an elliptical 52.5×25 nm^2 MTJ with a composite free layer. The magnetization of the left and right halves is shown separately.

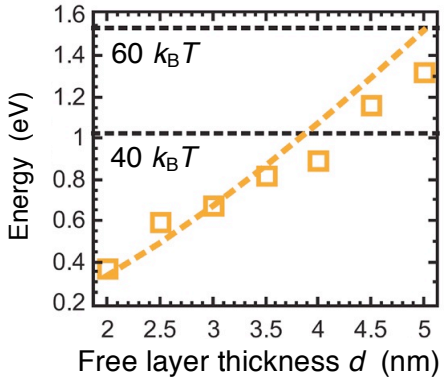

Figure 7. Thermal energy (dashed lines) *vs.* switching energy barriers (symbols) for MTJs with a composite free layer and 52.5×10 nm^2 cross-section as a function of the free layer thickness *d*. Each point is a result of statistical averaging with respect to 30 different realizations of the switching process.

- *Switching time*

The equality of the switching and the thermal barriers in composite structures results in an almost linear increase of the switching time in these MTJs with increasing thickness of the free layer and/or aspect ratio, see Fig. 8(a). A similar dependence is shown in Fig. 8(b) for a monolithic structure.

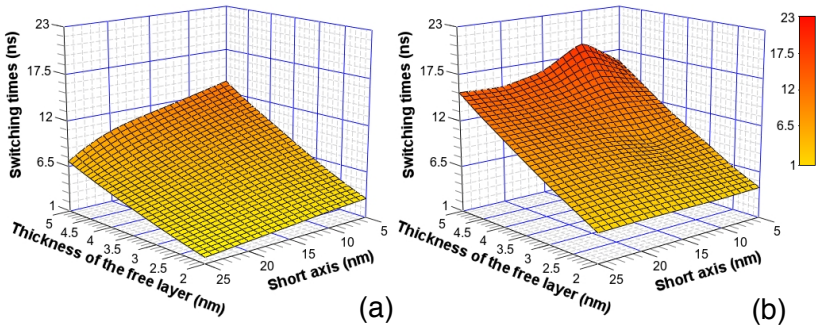

Figure 8. Switching times in the composite structure (a) and a monolithic structure (b) as a function of the thickness of the free layer and short axis length. The long axis is fixed at 52.5 nm and the thicknesses of the fixed layers are 5 nm.

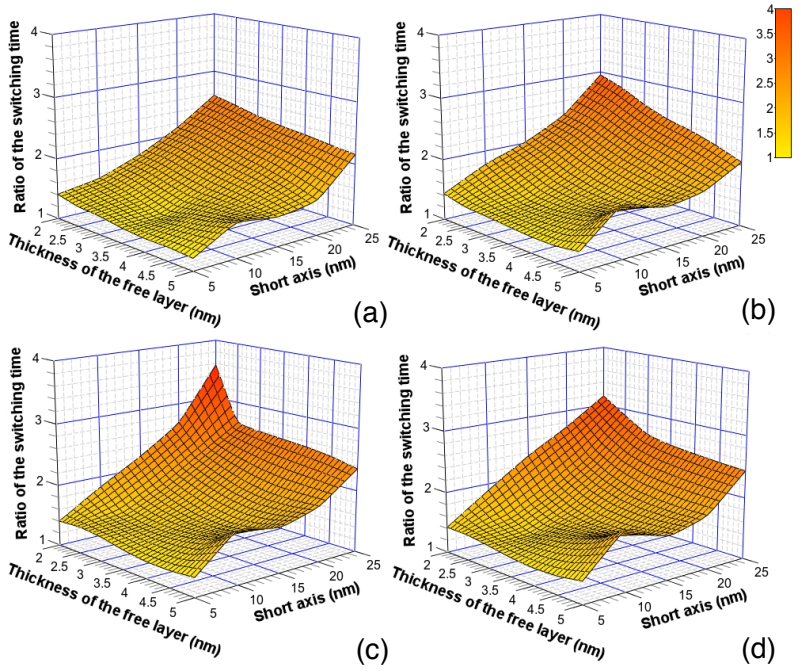

Figure 9. Switching time ratio between the monolithic and composite structures *vs.* free layer thickness and short axis length. The long axis is fixed at 52.5 nm. Dependences are shown for the thickness of the fixed layers: 5 nm (a), 10 nm (b), 15 nm (c), and 20 nm (d).

The influence of the MTJ geometry on the switching acceleration in MTJs with a composite free layer relative to the one with a monolithic layer is illustrated in Fig. 9. The long axis is fixed at 52.5 nm. Each point is a result of statistical averaging over 30 different realizations of the switching process. To decrease the switching time in the composite structure it is necessary to increase the thickness of the pinned layers. An almost threefold reduction of the switching time is achieved in MTJs with a composite free layer without compromising the thermal stability.

4. Conclusions

As in p-MTJs, in MTJs with a composite free layer the switching barrier energy is practically equal to the thermal stability barrier. Due to the removal of the central region in the monolithic structure, the shape anisotropy is slightly decreased together with the thermal stability factor. To boost the thermal stability factor in composite structures it is sufficient to increase the thickness of the free layer and/or the aspect ratio, so the thermal stability factor exceeds that for p-MTJs demonstrated to date. We have simulated an almost threefold decrease of the switching time in such structures. Therefore, the investigated MTJs offer considerable potential for performance optimization of STT-MRAM devices.

Acknowledgments

This research is supported by the European Research Council through the grant #247056 MOSILSPIN.

References

1. S. Hong, "Memory technology trend and future challenges," *Tech. Dig. IEDM* (2010), p. 292.
2. A. Makarov et al., "Emerging memory technologies: Trends, challenges, and modeling methods," *Microelectronics Reliability* **52**, 628 (2012).
3. S. S. P. Parkin, M. Hayashi, and L. Thomas, "Magnetic domain-wall racetrack memory," *Science* **320**, 190 (2008).
4. J. Slonczewski, "Current-driven excitation of magnetic multilayers," *J. Magn. Magn. Mater.* **159**, L1 (1996).
5. L. Berger, "Emission of spin waves by a magnetic multilayer traversed by a current," *Phys Rev. B* **54**, 9353 (1996).
6. D. Apalkov, S. Watts, A. Driskill-Smith, E. Chen, Z. Diao, and V. Nikitin, "Comparison of scaling of in-Plane and perpendicular spin transfer switching technologies by micromagnetic simulation," *IEEE Trans. Magnetics* **46**, 2240 (2010).

7. R. Sbiaa, S. Y. H. Lua, R. Law, H. Meng, R. Ley, and H. K. Tan, "Reduction of switching current by spin transfer torque effect in perpendicular anisotropy magnetoresistive devices," *J. Appl. Phys.* **109**, 07C707 (2011).
8. H. Sato, M. Yamanouchi, K. Miure, *et al*., "Junction size effect on switching current and thermal stability in CoFeB/MgO perpendicular magnetic tunnel junctions," *Appl. Phys. Lett.* **99**, 042501 (2011).
9. A. Makarov, V. Sverdlov, D. Osintsev, and S. Selberherr, "Reduction of switching time in pentalayer magnetic tunnel junctions with a composite-free layer," *Phys. Stat. Solidi Rapid Res. Lett.* **5**, 420 (2011).
10. A. Makarov, V. Sverdlov, D. Osintsev, and S. Selberherr, "Fast switching in magnetic tunnel junctions with two pinned layers: Micromagnetic modeling," *IEEE Trans. Magnetics* **48**, 1289 (2012).
11. J. Slonczewski, "Currents, torques, and polarization factors in magnetic tunnel junctions," *Phys. Rev. B* **71**, 024411 (2005).